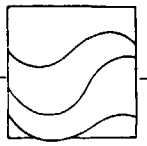

Currents
Countercurrents
Straits
Courants
Contre-courants
Détroits

Currents and countercurrents in straits

Ettore Salusti, Fabio Travaglioni
INFN, Dipartimento di Fisica, Università degli Studi « La Sapienza », Piazzale Aldo Moro 2, 00185 Roma, Italy.

Received 16/4/84, in revised form 23/11/84, accepted 3/12/84.

ABSTRACT

The steady inviscid motion of two superimposed homogeneous layers of sea water through a strait connecting two large, deep adjacent basins is discussed. A non-linear equation is obtained which can be linearized and solved by elementary functions, using scale analysis. As a simple application, the interface between "Atlantic" and "Levantine" water is computed for some western Mediterranean straits, *i.e.* Sardinia, Sicily and Corsica. In the case of the Corsica and Sicily channels, the results are in comforting agreement with known hydrological data. The Sardinia channel is interesting in that some of the model's hypotheses are violated. From a comparison with the hydrologic data it is thus possible to check their effective need. One particularly delicate aspect is the assumption of constant far-upstream potential vorticity since the presence of eddies, a frequent occurrence in real strait circulations, forbids the application of the model.

Oceanol. Acta, 1985, **8**, 2, 197-206.

RÉSUMÉ

Courants et contre-courants dans les détroits

On discute le mouvement stationnaire non visqueux de deux couches homogènes superposées d'eau de mer à travers un détroit connectant deux bassins adjacents grands et profonds. On obtient une équation non linéaire qui peut être linéarisée et résolue par des fonctions élémentaires, utilisant des arguments d'analyse d'échelle. Comme application simple, l'interface entre eau « atlantique » et eau « levantine » est calculée pour certains détroits de Méditerranée occidentale, notamment ceux de Sardaigne, de Sicile et de Corse. Dans le cas des détroits de Corse et de Sicile, les résultats sont en accord encourageant avec les données hydrologiques. Le détroit de Sardaigne est intéressant en ce sens que certaines hypothèses du modèle sont violées. Une comparaison avec les données hydrologiques permet donc de vérifier leur nécessité. Un aspect particulièrement délicat est l'hypothèse d'une vorticité potentielle constatée loin en amont, puisque la présence de tourbillons, qui apparaissent fréquemment dans les circulations des détroits réels, interdit l'application du modèle.

Oceanol. Acta, 1985, **8**, 2, 197-206.

INTRODUCTION

Steady inviscid currents flowing in two superimposed layers through a marine strait are discussed in this paper. Straits connecting large, deep basins are a common geographical feature throughout the world, particularly in the Mediterranean Sea. Water crossing straits can have a strong influence on the oceanographic characteristics of neighbouring basins. Defant (1961) studied several straits, coming to the conclusion that the dynamic origin of these steady currents lies in the temperature-salinity differences between adjoining basins. A classical example is the Strait of Gibraltar where a superficial flow of "Atlantic" water enters the Mediterranean, and is partly compensated for by a counterflow of heavier "Levantine" water in a deeper layer. However, this situation can be changed by winds and tides (Lacombe, 1971).

The first problem to solve in schematizing these phenomena is the determination of the steady inviscid motion of the two layers through the strait.

Whitehead, Leetmaa and Knox's study (1974) is particularly interesting in this regard. They assumed that the basins were very deep, which implied zero far-upstream asymptotic vorticity for the motion of the two layers. The resulting equations afforded solutions in terms of elementary functions: the transversal profile of the "interface" and the two fluxes were computed. The

along-strait profile of the interface was computed using a variational principle, *i.e.* by imposing the hydraulic principle of maximum transport in flow. The same kind of problem is discussed in Gill's (1977) study on sub/supercritical barotropic flows in geophysical straits. The "far-upstream" potential vorticity is assumed to be constant but not zero. The cross-strait velocity profile is described by a second-order differential equation. The longitudinal profile is computed by imposing that the two streamlines, identified by the intersections of the air-sea surface with the two banks of the strait, obey the Bernoulli equation. Significantly, barotropic countercurrents are allowed by this formulation.

Rydberg (1980) discussed critical flows for wide channels with strong variations in interface height along the flow. Frictional effects inside the channel are taken into account in this theory. Nof (1978 *a*; *b*) introduced a frictionless non-linear model to describe motion far from a state of geostrophic balance. The emphasis was laid on the study of a two-layer system.

The model examined in the present paper refers to steady inviscid motion of two superimposed layers through a marine strait in f_0 approximation. The two potential vorticity equations and the Bernoulli equations are obtained from fundamental physical principles.

Since non-linear effects are taken into account, our method is less restrictive than in the usual dynamic control technique. Applying scale analysis, a series expansion is obtained in which the first-order equation is still non-linear. But if the mouth of the strait is fairly large, a linear equation is obtained that can be solved by elementary functions (*see* next paragraph). This equation describes the transversal profile of the interface between the two layers. Significantly, this equation is mathematically equivalent (although with $g \to g'$) to the equation used by Gill (1977) to obtain the transversal profile of the air-sea interface. The along-strait profile is obtained from the Bernoulli equations as applied to the two streamlines corresponding to the intersection of the interface with the two banks (*see* third paragraph).

By way of application, the interface between surface Atlantic and intermediate Levantine water is computed for some western Mediterranean straits, *i.e.* Sardinia, Sicily, Corsica (*see* fourth paragraph). In the case of the Corsica and Sicily channels, a reasonable agreement is obtained between our results and known hydrological data. The Sardinia channel is interesting since the model's hypotheses are not fulfilled. It is thus possible to check their effective need. The constant far-upstream potential vorticity hypothesis is particularly delicate since the presence of eddies, frequently occurring in real straits, forbids the application of the model.

This study generalizes a preceding analysis by Colacino *et al.* (1981) in which barotropic effects were considered. Since the two layers are clearly detectable throughout the Mediterranean Sea, here we have been obliged to take baroclinic effects into account. Moreover, this study differs from the model of Gill and Schumann (1979, to study the Agulhas Current) and from the application of Hogg (1983, to study the Vema Channel), in that we do not *a priori* assume geostrophic balance in the cross-strait direction.

THE MODEL

We now discuss the velocity field for the steady motion of two superimposed, homogeneous layers of sea water (densities ρ_1 and ρ_2, $\rho_2 > \rho_1$) through a strait connecting two adjoining basins, *i.e.* large, deep reservoirs. Figure 1 shows the general hydrological situation: $d_i(x, y)$ (with $i=1, 2$) are the layer depths, $D(x, y)$ the bottom depth, $\xi = d_1 + d_2 - D$ is the surface elevation and x and y are the along-strait and cross-strait coordinates, respectively; z (directed upward) is the depth, f_0 is the Coriolis parameter, assumed to be constant, and $V_i \equiv (u_i, v_i)$, $i=1,2$, are the horizontal steady velocities for the two layers. The channel is long, fairly flat and lies between $x = L(y)$ and $x = -L(y)$. Friction and mixing are neglected. For each layer ($i=1,2$) the continuity equation gives

$$\partial_x (d_i u_i) + \partial_y (d_i v_i) = 0. \tag{1}$$

The stream functions $\psi_i(x, y)$ are

$$\partial_x \psi_i = d_i v_i, \qquad -\partial_y \psi_i = d_i u_i. \tag{2}$$

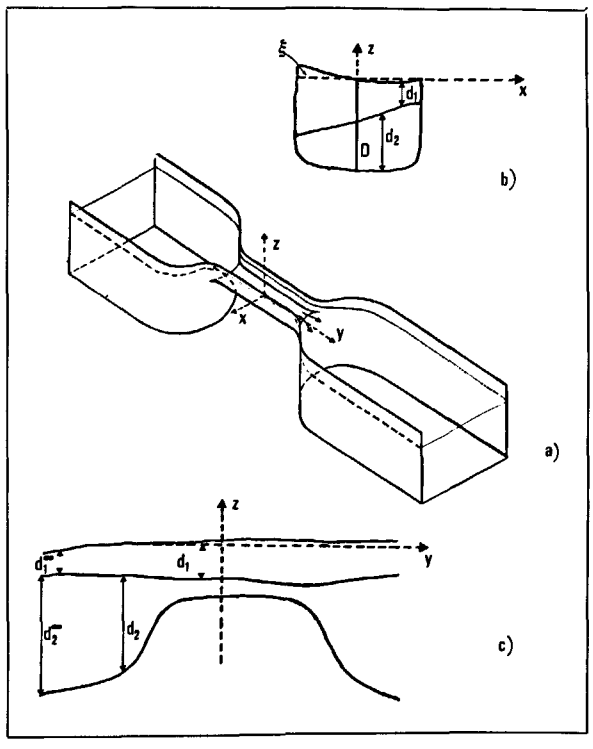

Figure 1
Description of the symbols used in the theoretical discussion: a) general view; b) cross-stream section; c) along-stream section.

The dynamic equations can be written in the form

$$\begin{aligned} -(f_0 + \omega_i) v_i &= -\partial_x G_i(\psi_i) \\ (f_0 + \omega_i) u_i &= -\partial_y G_i(\psi_i), \end{aligned} \tag{3}$$

where $\omega_i \equiv (\partial_x v_i - \partial_y u_i)$ is the relative vorticity and

$$G_1(\psi_1)=g\xi+\frac{1}{2}\left(\frac{1}{d_1}\nabla\psi_1\right)^2$$
$$G_2(\psi_2)=g\xi-g'd_1+\frac{1}{2}\left(\frac{1}{d_2}\nabla\psi_2\right)^2 \quad (4)$$

are the Bernoulli functions for both layers, with $g'\equiv g(\rho_2-\rho_1)/\rho_2$. From (3), we obtain the potential vorticity equation (Charney, 1955)

$$\frac{f_0+\omega_i}{d_i}=F_i(\psi_i)\equiv\frac{d}{d\psi_i}G_i(\psi_i). \quad (5)$$

To determine the unknown functions $F_i(.)$ and $G_i(.)$ we remark that far upstream $|\omega|\equiv|\partial_x v_1-\partial_y u_1|\ll f_0$. We therefore assume that

$$\lim_{y\to-\infty}\omega_1\equiv\lim_{y\to-\infty}(\partial_x v_1-\partial_y u_1)=0. \quad (6)$$

From (5) we obtain

$$F_1(\psi_1)=\lim_{y\to-\infty}f_0/d_1\equiv f_0/d_1^\infty\equiv A_1 \quad (7)$$

and

$$G_1(\psi_1)=f_0/d_1^\infty\psi_1+g\xi^\infty\equiv A_1\psi_1+B_1 \quad (8)$$

where $\chi^\infty\equiv\lim_{y\to-\infty}\chi$.

For the lower layer, using the same assumption (although the current is flowing in the opposite direction) we obtain

$$F_2(\psi_2)=\lim_{y\to\infty}f_0/d_2\equiv f_0/d_2^\infty\equiv A_2 \quad (9)$$

and

$$G_2(\psi_2)=(\lim_{y\to\infty}f_0/d_2)\psi_2+\lim_{y\to\infty}(g\xi-g'd_1)$$
$$\equiv f_0/d_2^\infty\psi_2+g\xi^\infty-g'd_1^\infty\equiv A_2\psi_2+B_2. \quad (10)$$

The assumption of constant potential vorticity is discussed by Whitehead (1974) and Gill (1977).
The resulting equations are

$$\frac{1}{d_1}\left\{f_0+\nabla\left(\frac{1}{d_1}\nabla\psi_1\right)\right\}=f_0/d_1^\infty\equiv A_1$$
$$g\xi+\frac{1}{2}\left(\frac{1}{d_1}\nabla\psi_1\right)^2=f_0/d_1^\infty\psi_1+g\xi^\infty\equiv A_1\psi_1+B_1$$
$$\frac{1}{d_2}\left\{f_0+\nabla\left(\frac{1}{d_2}\nabla\psi_2\right)\right\}=f_0/d_2^\infty\equiv A_2$$
$$g\xi-g'd_1+\frac{1}{2}\left(\frac{1}{d_2}\nabla\psi_2\right)^2=\frac{f_0}{d_2}\psi_2+g\xi^\infty-g'd_1^\infty\equiv A_2\psi_2+B_2$$
$$D=d_1+d_2-\xi, \quad (11)$$

where $\nabla\equiv(\partial_x,\partial_y)$. Using a scale analysis of these non-linear equations, it is easy to show (Table) that the preceding set of non-linear equations can naturally be approximated by

Table
Scale values for the physical quantities appearing in our equations, as evaluated from a consideration of the western Mediterranean straits.

$\bar{x}\sim10^4$ m
$\bar{y}\sim10^6$ m
$\bar{u}_i\sim10^{-3}$ ms^{-1}
$\bar{v}_i\sim10^{-1}$ ms^{-1}
$\bar{\xi}\sim10^{-1}$ m
$\xi^\infty\sim10^{-2}\div10^{-3}$ m
$f_0\sim10^{-4}$ s^{-1}
$\bar{Q}\sim10^5$ m^3 s^{-1}
$\partial_x\bar{v}_i-\partial_y\bar{u}_i\sim10^{-5}$ s^{-1}
$f_0\bar{d}_1/d_1^\infty\sim10^{-4}$ s^{-1}
$g\bar{\xi}\sim g'\bar{d}_1\sim1$ m^2 s^{-2}
$f_0\bar{Q}/d_1^\infty\sim10^{-1}$ s^{-2}
$g\xi^\infty\sim10^{-1}\div10^{-2}$ s^{-2}
$\bar{d}_1\sim d_1^\infty\sim10^2$ m
$\bar{d}_2\sim d_2^\infty\sim10^3$ m
$\frac{1}{2}(\bar{u}^2+\bar{v}^2)\sim10^{-2}$ m^2 s^{-2}

$$f_0+\frac{d}{dx}\left\{\frac{1}{d_1}\frac{d}{dx}\psi_1\right\}\cong A_1 d_1$$
$$A_1\psi_1\cong g(\xi-\xi^\infty)+\frac{1}{2}\left(\frac{1}{d_1}\nabla^2\psi_1\right)^2$$
$$f_0+\frac{d}{dx}\left\{\frac{1}{d_2}\frac{d}{dx}\psi_2\right\}\cong A_2 d_2$$
$$g(\xi-\xi^\infty)-A_2\psi_2\cong g'(d_1-d_1^\infty)-\frac{1}{2}\left(\frac{1}{d_2}\nabla\psi_2\right)^2$$
$$D=d_1+d_2-\xi \quad (12)$$

in the unknowns ψ_1, ψ_2, d_1, d_2, ξ. The terms with y derivatives are smaller than other terms by a factor of 10^{-4}. They have therefore been disregarded.
Let us now remark that the v_1^2, v_2^2 terms are $\sim10^{-1}$ times the other terms in the Bernoulli equations and moreover that $v_1^2(y)\sim v_2^2(y)$ since they are of the same magnitude and have the same behaviour. Moreover $A_2/A_1\sim10^{-1}$; then

$$g'(d_1-d_1^\infty)=A_1\psi_1-A_2\psi_2+\frac{1}{2}\left(\frac{1}{d_2}\nabla\psi_2\right)^2-\frac{1}{2}\left(\frac{1}{d_1}\nabla\psi_1\right)^2\sim f_0\frac{\psi_1}{d_1^\infty}$$

At worst, our approximation is ~10 %; *i.e.* comparable with the uncertainty of the hydrologic data. It then results that

$$\frac{d}{dx}\left\{\frac{1}{d_1}\frac{d}{dx}d_1\right\}=\frac{f_0^2}{g'd_1^\infty}\left(\frac{d_1}{d_1^\infty}-1\right)\equiv R^{-2}\left(\frac{d_1}{d_1^\infty}-1\right) \quad (13)$$

in which R is the Rossby internal deformation radius. If the quantity $d_1/d_1^\infty\simeq1$, *i.e.* for deep straits, we obtain

$$\frac{d}{dx}\frac{1}{d_1}\frac{d}{dx}d_1=\frac{d^2}{dx^2}\ln\frac{d_1}{d_1^\infty}\simeq\frac{d^2}{dx^2}\frac{d_1}{d_1^\infty}=R^{-2}\left(\frac{d_1}{d_1^\infty}-1\right). \quad (15)$$

Moreover, for large straits the velocities on the sill are not as great as for narrow straits. Therefore the inclination of the interface is small and this $d_1/d_1^\infty \sim 1$ position can be verified. This equation is mathematically equivalent to that obtained by Gill (1977) to describe the air-sea interface in the case of barotropic flows, with $g \to g'$. The solutions are

$$d_1(x, y) = d_1^\infty + a(y) \cosh \frac{x}{R} + b(y) \operatorname{senh} \frac{x}{R} \tag{16}$$

$$\psi_1(x, y) = \frac{g' d_1^\infty}{f_0} \left\{ a(y) \cosh \frac{x}{R} + b(y) \operatorname{senh} \frac{x}{R} \right\} \tag{17}$$

$$\xi(x, y) = \xi^\infty + \frac{g'}{g} \left\{ a(y) \cosh \frac{x}{R} + b(y) \operatorname{senh} \frac{x}{R} \right\}. \tag{18}$$

In the case of geostrophic balance, the velocity is given by

$$v_1(x, y) \simeq \frac{g'}{f_0} \partial_x d_1 = \frac{g'}{f_0 R} \times \left\{ a(y) \operatorname{senh} \frac{x}{R} + b(y) \cosh \frac{x}{R} \right\}. \tag{19}$$

The profiles of d_1, ψ_1, ξ, v_1 have a rather simple shape and depend on the $a(y)$, $b(y)$ variables. Intuitively, they are exponentially decreasing functions with maxima at the banks.

THE ALONG-STRAIT PROFILE

The unknowns $a(y)$ and $b(y)$ can be obtained from the two boundary conditions on $x = \pm L(y)$, *i.e.* on the banks of the strait. More precisely, let us take two streamlines of the upper layer, very near the intersection of the interface with the right and left banks, $x = \pm L(y)$ (Gill, 1977).
The Bernoulli equations give

$$\begin{aligned} &g\xi + \frac{1}{2}\left(\frac{1}{d_1} \nabla \psi_1\right)^2 \Big|_{\text{right bank}} \\ &\quad = g\xi_r^\infty + \frac{f_0}{d_{1r}^\infty} \psi_1 \Big|_{\text{right bank}} \\ &g\xi + \frac{1}{2}\left(\frac{1}{d_1} \nabla \psi_1\right)^2 \Big|_{\text{left bank}} \\ &\quad = g\xi_l^\infty + \frac{f_0}{d_{1l}^\infty} \psi_1 \Big|_{\text{left bank}}, \end{aligned} \tag{20}$$

where in $\xi_{r(l)}^\infty$ and $d_{1r(l)}^\infty$ the raising of the air-sea surface and the interface on the right (left) bank of the upstream basin is taken into consideration. For the right bank ($x = L(y)$) it is found that

$$\xi^\infty - \xi_r^\infty = \frac{\Delta\rho}{\rho} \left\{ -\frac{1}{2 d_1^\infty} \left(a \operatorname{senh} \frac{L}{R} + b \cosh \frac{L}{R} \right)^2 + \left(\frac{d_1^\infty}{d_{1r}^\infty} - 1 \right) \left(a \cosh \frac{L}{R} + b \operatorname{senh} \frac{L}{R} \right) \right\} \tag{21}$$

and for the left bank ($x = -L(y)$)

$$\xi^\infty - \xi_l^\infty = \frac{\Delta\rho}{\rho} \left\{ \frac{1}{2 d_1^\infty} \left(a \operatorname{senh} \frac{L}{R} - b \cosh \frac{L}{R} \right)^2 + \left(\frac{d_1^\infty}{d_{1l}^\infty} - 1 \right) \left(a \cosh \frac{L}{R} - b \operatorname{senh} \frac{L}{R} \right) \right\}. \tag{22}$$

The quantities $a(y)$ and $b(y)$ can easily be derived for special cases (a more complete discussion is in the Appendix):
1) We first consider barotropic motion, in formulae defined by $d_1^\infty = d_l^\infty = d_r^\infty$. We assume that d_1^∞, ξ^∞, $L(y)$ and the flux of the upper layer $Q_1 = \psi_r - \psi_l$ are given. We thus compute ξ, v_1, d_1. If $\xi_1^\infty = \xi^\infty$, the entire flow enters the strait. Equations (21), (22) give

$$\begin{aligned} &a \operatorname{senh} \frac{L}{R} = b \cosh \frac{L}{R} \\ &\frac{1}{2} \frac{\Delta\rho}{\rho} \left(a \operatorname{senh} \frac{L}{R} + b \cosh \frac{L}{R} \right)^2 \\ &= 2 \frac{\Delta\rho}{\rho} b^2 \cosh^2 \frac{L}{R} = -d_1^\infty (\xi^\infty - \xi_r^\infty). \end{aligned} \tag{23}$$

One thus obtains

$$a \operatorname{senh} \frac{L}{R} = b \cosh \frac{L}{R} = \pm \sqrt{\frac{1}{2} \frac{\rho}{\Delta\rho} d_1^\infty (\xi_r^\infty - \xi^\infty)} \tag{24}$$

The flux Q through the strait is given by

$$\begin{aligned} Q_1 &= \int_{-L}^{L} d_1 v_1 \, dx = \int_{-L}^{L} \frac{d}{dx} \psi \, dx = \psi \Big|_{\text{left bank}}^{\text{right bank}} \\ &= 2 \frac{g' d_1^\infty}{f_0} b \operatorname{senh} \frac{L}{R} \equiv Q_1^\infty \operatorname{tgh} \frac{L}{R} \end{aligned} \tag{25}$$

Defining

$$Q_1^\infty = \pm \sqrt{\frac{2 d_1^\infty \Delta\rho}{\rho} (\xi_r^\infty - \xi^\infty)} \frac{g d_1^\infty}{f_0} \tag{26}$$

We have

$$\begin{aligned} d_1 &= d_1^\infty + \frac{Q_1^\infty}{2 f_0 R^2} \left[\frac{\cosh x/R}{\operatorname{senh} L/R} + \frac{\operatorname{senh} x/R}{\cosh L/R} \right] \\ &= d_1^\infty + \frac{Q_1^\infty}{f_0 R^2} \frac{\operatorname{ch}((x+L)/R)}{\operatorname{sh}(2L/R)} \\ \xi &= \xi^\infty + \frac{Q_1^\infty f_0}{g d_1^\infty} \frac{\operatorname{ch}((x+L)/R)}{\operatorname{sh}(2L/R)} \\ v &= \frac{Q_1^\infty}{2 R d_1^\infty} \left[\frac{\operatorname{senh} x/R}{\operatorname{senh} L/R} + \frac{\cosh x/R}{\cosh L/R} \right] \\ &= \frac{Q_1^\infty}{R d_1^\infty} \frac{\operatorname{sh}((x+L)/R)}{\operatorname{sh}(2L/R)}. \end{aligned} \tag{27}$$

Other cases can be treated in a similar way.
2) Baroclinic motion, schematized as $\xi^\infty = \xi_r^\infty = \xi_l^\infty$. Given d_1^∞, ξ^∞, $L(y)$ and the fluxes Q_1 and Q_2 we compute ξ_1, d_1 and v. It should be noted that since $\xi_r^\infty = \xi^\infty = \xi^\infty$, the total flux is zero and $Q_1 = -Q_2$. If

$d_r^\infty - d_1^\infty \sim d_1^\infty - d_l^\infty > 0$, one is dealing with a flow of the upper layer which is compensated by a counterflow in the lower layer, a rather frequent occurrence in the Mediterranean Sea. From (21), (22) one thus obtains

$$\left(a \operatorname{senh}\frac{L}{R} + b\cosh\frac{L}{R}\right)^2 = \theta\left(a\cosh\frac{L}{R} + b\operatorname{senh}\frac{L}{R}\right)$$

$$\left(a \operatorname{senh}\frac{L}{R} - b\cosh\frac{L}{R}\right)^2 = \theta\left(b\operatorname{senh}\frac{L}{R} - a\cosh\frac{L}{R}\right) \qquad (28)$$

where

$$\theta \equiv \left(\frac{d_1^\infty}{d_{1r}^\infty} - 1\right) 2 d_1^\infty$$

This implies that

$$b(y) = \frac{\theta}{2}\frac{1}{\operatorname{senh}(L/R)}$$

$$a(y) = \frac{\pm\theta}{2\operatorname{sh}(L/R)}\sqrt{2 - \operatorname{cotgh}^2(L/R)} \qquad (29)$$

positive if $L > 0.89\,R$.

Defining

$$Q_1 = -Q_2 = \frac{2g' d_1^{\infty 2}}{f_0}\left(\frac{d_1^\infty}{d_{1r}^\infty} - 1\right) = \tilde{Q}^\infty, \qquad (30)$$

as result we can obtain the velocities and air-sea elevations:

$$d_1 - d_1^\infty = \frac{\tilde{Q}^\infty}{2 f_0 R^2 \operatorname{senh} L/R} \times \left\{\pm\sqrt{2 - \operatorname{cotgh}\frac{L}{R}}\cosh\frac{x}{R} + \operatorname{senh}\frac{x}{R}\right\}$$

$$\simeq \frac{\tilde{Q}^\infty}{2 f_0 R^2 \operatorname{senh} L/R} \times \left(\pm\cosh\frac{x}{R} + \operatorname{senh}\frac{x}{R}\right)$$

$$\xi - \xi^\infty = \frac{\tilde{Q}^\infty \Delta\rho}{2\rho f_0 R^2 \operatorname{senh} L/R} \times \left\{\pm\sqrt{2 - \operatorname{cotgh}\frac{L}{R}}\cosh\frac{x}{R} + \operatorname{senh}\frac{x}{R}\right\} \qquad (31)$$

$$\simeq \frac{Q^\infty \Delta\rho\, \tilde{Q}^\infty}{2\rho f_0 R^2 \operatorname{senh} L/R}\left(\pm\cosh\frac{x}{R} + \operatorname{senh}\frac{x}{R}\right)$$

$$v = \frac{\tilde{Q}^\infty}{2 R d_1^\infty \operatorname{senh} L/R} \times \left\{\pm\sqrt{2 - \operatorname{cotgh}\frac{L}{R}}\operatorname{senh}\frac{x}{R} + \cosh\frac{x}{R}\right\}$$

$$\simeq \frac{\tilde{Q}^\infty}{2 R d_1^\infty \operatorname{senh} L/R} \times \left(\pm\operatorname{senh}\frac{x}{R} + \cosh\frac{x}{R}\right).$$

These results are used in the discussion of several western Mediterranean straits.

Let us now examine a pathology of our model. For barotropic motions, from equation (25) it follows that the flux $Q \simeq \operatorname{tgh} L/R$. It can easily be deduced that the flux is greater in the upstream basin than on the strait sill. This regrettable pathology is probably due to the errors resulting from the scale analysis.

APPLICATION TO SEVERAL WESTERN MEDITERRANEAN STRAITS

The Mediterranean Sea is divided into numerous basins linked by straits or channels (Defant, 1961; Colacino *et al.*, 1981). The water exchange between the various basins can be estimated by hydrological analysis. In this section the effectiveness of our model is tested on some western Mediterranean straits, *i.e.* the Straits of Sicily, Sardinia and Corsica. However, some care must be taken in making this kind of comparison. For instance, it is a known fact that the irregularity of the bottom depth of real straits can give rise to peculiar effects, *e.g.* non-linear phenomena, friction, eddies, *etc.* In the Mediterranean Sea, in particular, friction is an important factor and the mixing of water from different layers can give rise to effects observable over a wide area. Some of these effects will be examined in greater detail in the following.

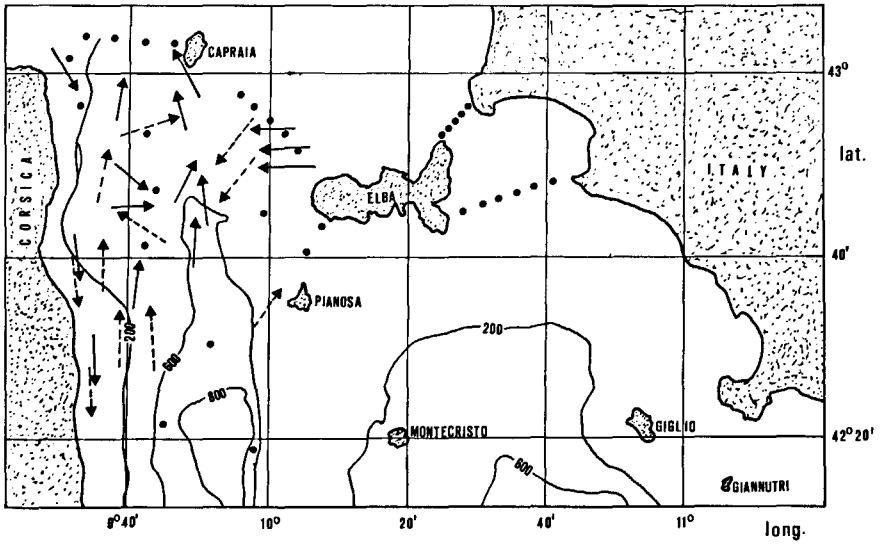

Figure 2
Bottom topography in the Corsica channel. Depth in meters. Hydrological sections, ○, surface → and deep layer ⇢ velocities are also shown (from Stocchino, Testoni, 1969).

The Corsica channel

The Corsica channel comprises the sea area lying between the Ligurian and Tyrrhenian seas off the Corsican and Tuscan coasts. It also includes the islands of Elba, Capraia and Pianosa, *etc.* in the Tuscan Archipelago (Fig. 2).

The channel may be subdivided into two branches. The first branch lies between Corsica and the islands, the second between the islands and Tuscany. The first branch reaches a depth of 453 m and contributes most of the water flux between the two seas. Stocchino and Testoni (1969) observed a surface flow (running northward between Corsica and the islands of Capraia, Montecristo and Pianosa) and a countercurrent near Corsica. This pattern is altered by the water flux from the Elba channel (lying between Elba and Capraia), which splits into two branches, the first of which flows northward after skirting Capraia, and the second which interacts with the main stream, forming a cyclonic eddy. At a lower level the interaction with the bottom irregularities produces a different pattern from that at the surface; the eddy, again present, rotates clockwise (Fig. 2). In the deepest part, the measurements show a more regular flux of cold water directed northward. The hydrology of the different sections is shown in Figure 3 *a*, *b*. The interface is related to temperature gradients, *i.e.* the 14°C isothermals.

Since the water motion of the two layers is fairly coherent, equation (27) is used in which

$$Q^{\infty} = 7.10^{5}\ \mathrm{m^3/s}$$
$$f_0 = 10^{-4}\ \mathrm{s^{-1}}$$
$$g' = 2.10^{-3}\ \mathrm{m/s^2}$$
$$d_1^{\infty} = 120\ \mathrm{m}. \qquad (32)$$

The interface is shown in Figure 3 *a*, 3 *b*, and is in qualitative agreement with the 14°C isothermals.

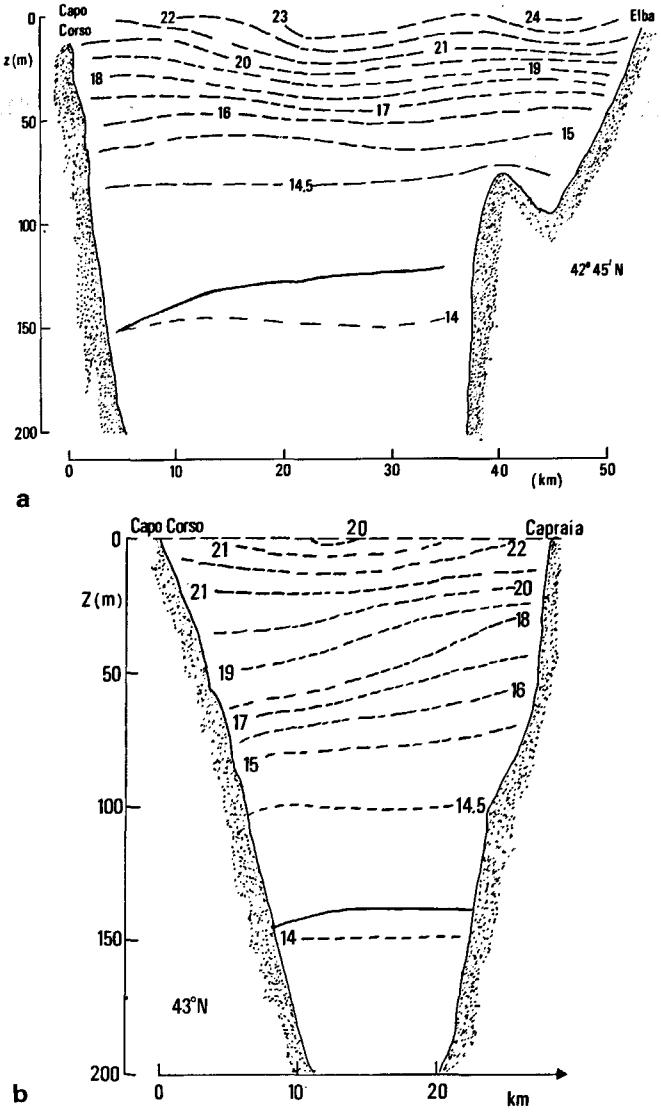

Figure 3

Temperature profiles in the Corsica channel along 2 vertical sections: a) 42°45′ N; b) 43°N. —— temperature experimental data were taken from Stocchino et al. *(1969); —— theoretical values were computed using our "barotropic" equations.*

The Sicily Channel

The Sicily channel is the critical region of water exchange between the eastern and western Mediterranean basins. The circulation has been studied in detail by Garzoli and Maillard (1978) and by Garzoli *et al.* (1981). It is mainly dependent on the complex bottom topography (Frassetto, 1964; Fig. 4). The continental

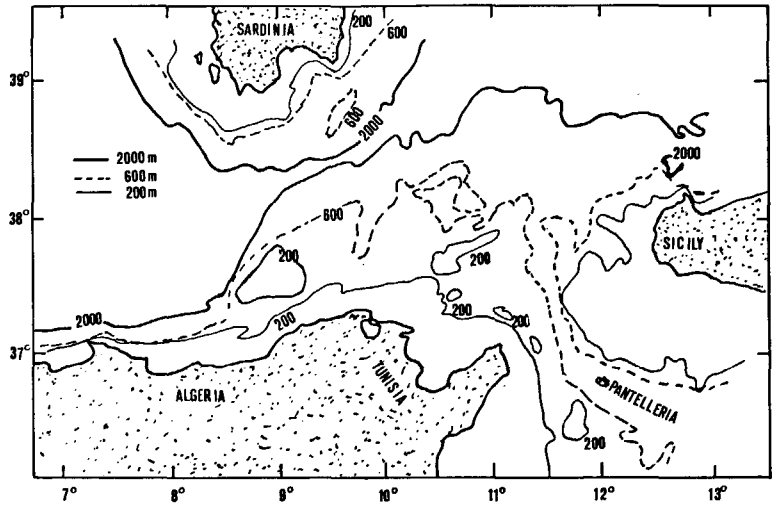

Figure 4

Bottom topography in the Sicily and Sardinia channels. Depths in fathoms (after Garzoli, Maillard, 1978).

shelf is fairly wide along both coasts. Near the level of the Intermediate Levantine layer, the eastern and western basins of the Mediterranean communicate mainly through two complex channels. The deeper of these channels (430 m, on the sill) runs northwards, while the other (365 m, on the sill) runs northwest.

A two-layer system is evident in the Sicilian Ridge. On the bottom there is a flux mainly composed of Levantine water (with a local salinity of 38.75°/$_{oo}$). The 38.0 isohaline has been chosen as the interface. Using the dynamic method, Garzoli and Maillard (1978; *see* also Morel, 1969) estimated an incoming flux of 10^6 m^3/s. Outside the channels, communication between the basins is partially obstructed so that the Intermediate Levantine water is obliged to flow along the channels toward the North. Figure 5 points to the presence of countercurrents related to the baroclinic properties of the flow.

Since the water motion is baroclinic we can apply equation (31) with

$$Q^{\infty} = 1.3.10^6 \text{ m}^3/\text{s}$$
$$f_0 = 0.9.10^{-4} \text{ s}^{-1}$$
$$g' = 2.10^{-3} \text{ m/s}^2$$
$$d_1^{\infty} = 150 \text{ m}. \qquad (33)$$

The resulting pictures are shown in Figure 5 *a-d* and are in good qualitative agreement with the hydrological data. Apart from the ridge in Figure 5*a*, which is difficult to treat theoretically, the main discrepancy is due to the rather strong gradient of the theoretical interface near the African coast. Clearly, the $d_1 \sim d_1^{\infty}$ hypothesis is much weaker near the coast, where the non-linear terms come into play. This shows that our model cannot usefully be applied to small-mouth straits such as Gibraltar and Messina.

The Sardinia channel

The Sardinia channel is a narrow valley with an average maximum depth of about 2000 m (Fig. 4). A fairly wide continental shelf exists along both coasts. The hydrology clearly indicates that the Intermediate Levantine water is divided into two veins (Fig. 6*a*, *b*). The section drawn in the eastern part of the straits (8°52′E) shows that the layer of Intermediate water is almost continuous from North to South in the channel (Fig. 7*d*). At 7°48′E (Fig. 7*a*) in the western part of the strait, the Intermediate water is divided into two comparable veins. Geostrophic velocities are of the order of 5 cm/s westward in both veins. From the hydrological and dynamic analyses Garzoli and Maillard (1978) have concluded that the winter circulation is related to the existence of two eddies covering the surface and intermediate layers (up to 500 m). In the surface layer the main flux flows eastward between the two eddies. At Intermediate water level (Fig. 6*b*), the flux towards the West divides into two veins outside the two eddies, one along the North African coast, and the other along the southern coast of Sardinia. These

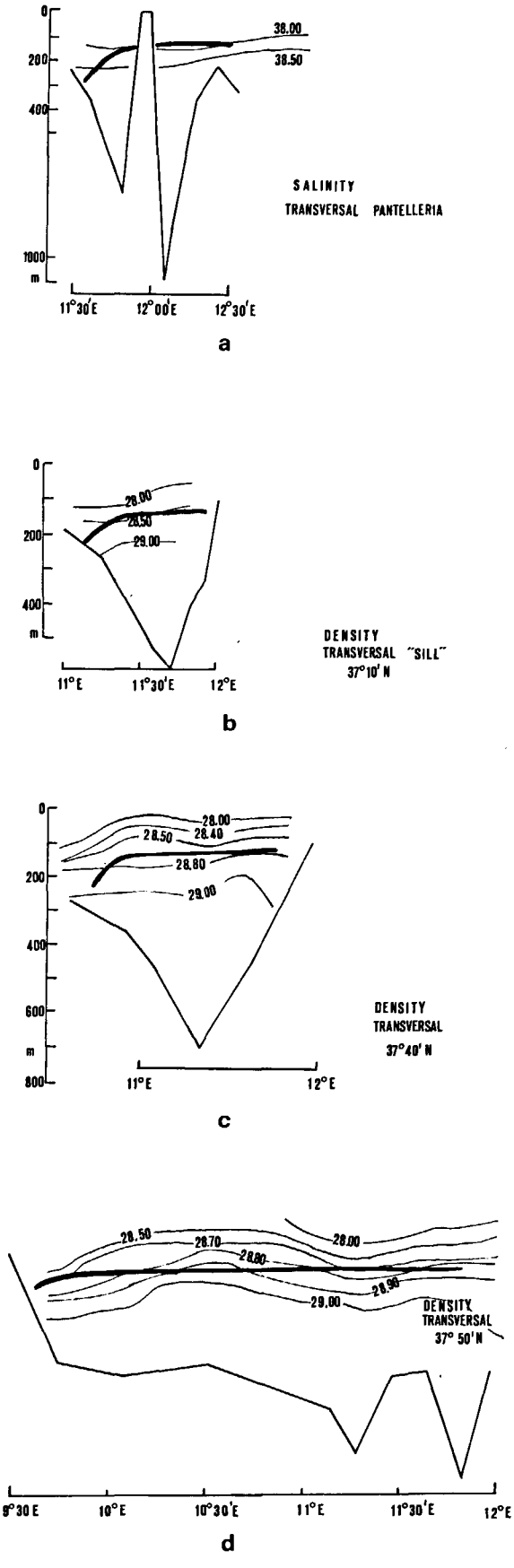

Figure 5

Density or salinity profiles in the Sicily channel along 4 vertical sections: a) the transversal containing the island of Pantelleria; b) the transversal on 37°10′ N; c) the transversal on 37°40′ N, d) the transversal on 37°50′ N. —— density or salinity experimental data were taken from Garzoli and Maillard (1978); ——*theoretical values came from our "baroclinic" equations.*

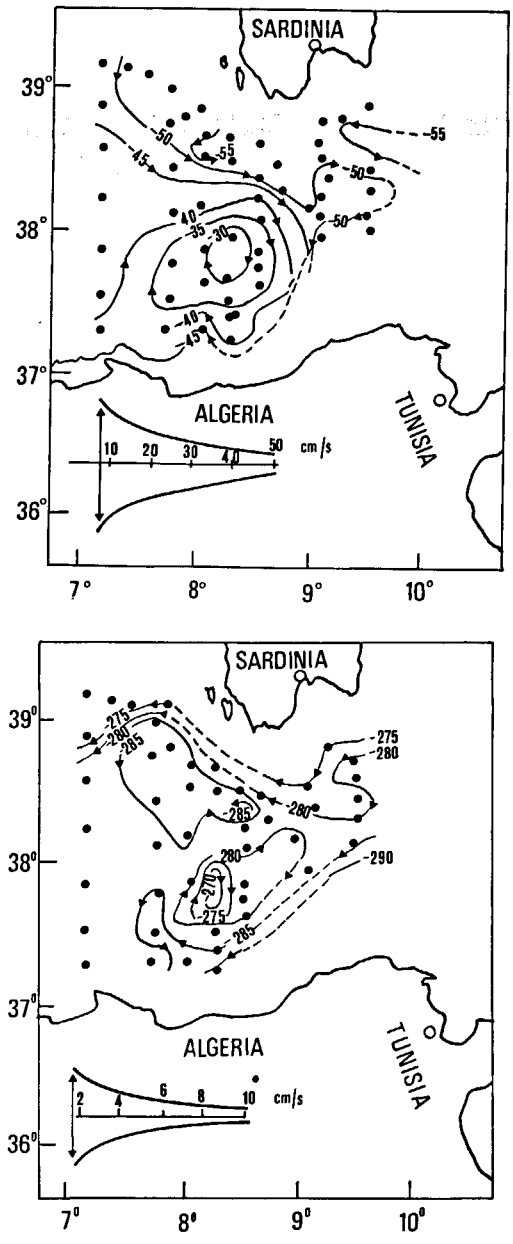

Figure 6
Surface (a) and deeper (b) layer circulation in the region of the Sardinia channel, from Garzoli and Maillard (1978).

eddies are not symmetric; in both layers the anticyclonic eddy is the more important.
Different values were found for the fluxes estimated from available data for the mouth and end of the Sardinia channel. Because of the continuity condition, if incoming surface water has a flux of about 10^6 m^3/s, an outgoing flux of the same order must be found for the intermediate water. However, in the latter case, it must be divided into two branches running parallel to the coasts. The reason for this is that countercurrents cannot be detected by means of dynamic analysis in the shallow coastal regions. The fluxes must, in any case, be located near the coasts.

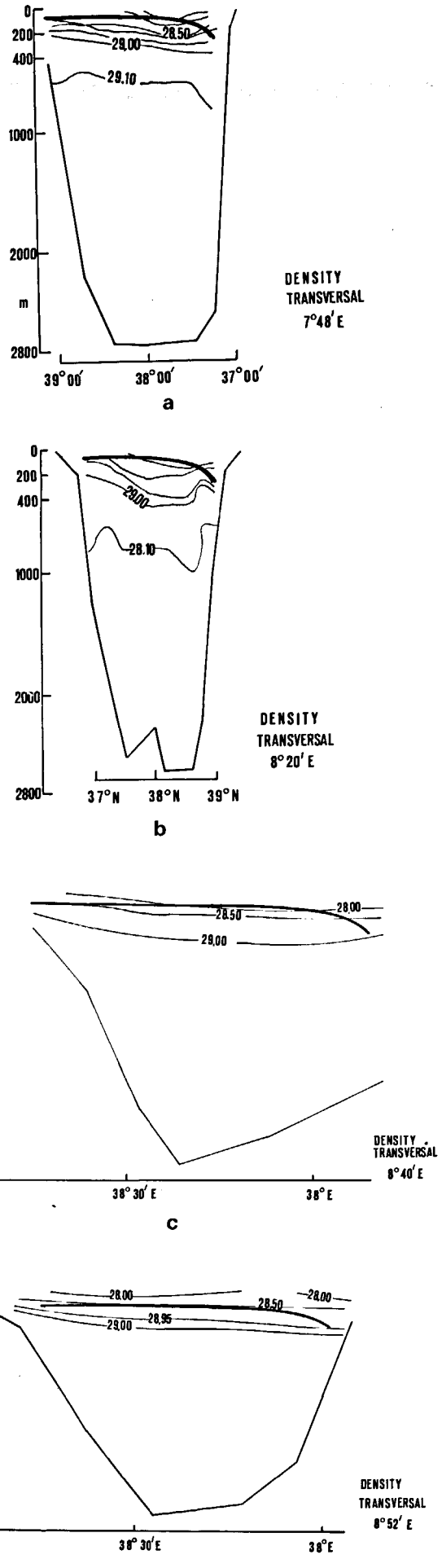

Figure 7
Density profiles in the Sardinia channel along 4 vertical sections: a) on 7°48′ E; b) on 8°20′ E; c) on 8°40′; d) on 8°52′. —— density experimental data were taken from Garzoli and Maillard (1978); —— *theoretical values came from our "baroclinic" equations.*

In this case one has:

$$Q^{\infty} = 10^6 \text{ m}^3/\text{s}$$
$$f_0 = 0.9 \cdot 10^{-4} \text{ s}^{-1}$$
$$g' = 2 \cdot 10^{-3} \text{ m/s}^2$$
$$d_1^{\infty} = 150 \text{ m}. \qquad (34)$$

The results are shown in Figure 7. Significantly, agreement is worse than in the case of the Sicily channel; this can probably be explained by the presence of the two eddies. In fact, a different theoretical model has been suggested by Garzoli and Maillard (1978) and Garzoli *et al.* (1981) :

$$\frac{\nabla \cdot (1/d_i) \nabla \psi_i + f_0}{d_i} = A_i \psi_i + B_i$$
$$A_i, B_i \in \mathbb{R}$$

with good results. Their model differed from ours in that the interface depth was obtained through observation and only streamlines were computed separately for the two layers. However, the vorticity was different: the $A_i \psi_i + B_i$ functional form cannot be obtained from our equations.

CONCLUSION

We examined the steady inviscid flow of two superimposed layers of sea water flowing through a strait connecting two large, deep, adjoining basins. The motion is governed by the conservation of potential vorticity and by the Bernoulli equation. Scale analysis is used to obtain a simple equation to describe the cross-strait shape of the interface between the two layers. This equation is mathematically equivalent to the one obtained by Gill (1977) for a barotropic flow, with $g \to g'$.

The application of these methods to the straits of Corsica, Sicily and Sardinia (western Mediterranean Sea) shows that the barotropic case gives good results (Corsica), while the baroclinic case gives good results in the case of the Sicily channel, where the hypothesis of constant far upstream potential vorticity is satisfied. In the case of the Sardinia channel, the hypothesis is violated and the agreement with the hydrological data is far worse.

Acknowledgements

We wish to thank Dr. Silvia Garzoli for helpful criticism and Dr. Massimo Abbate for many useful suggestions.

REFERENCES

Charney J., 1955. The Gulf Stream as an inertial boundary layer, *Proc. Nat. Acad. Sci.* **41**, 10, 731-740.
Colacino M., Garzoli S., Salusti E., 1981. Currents and countercurrents in the Western Mediterranean straits, *Nuovo Cimento C*, **4**, 123-144.
Defant A., 1961. *Physical oceanography*, Pergamon Press, Oxford, 2 vol., 730 and 570 p.
Frassetto R., 1964. A study of the turbulent flow and character of the water masses over the Sicilian Ridge in both summer and winter, *Rapp. PV CIESM*, **18**, 3, 812, p. 15.
Garzoli S., Maillard C., 1979. Winter circulation in the Sicily and Sardinia straits region, *Deep-Sea Res.*, **26**, 933-954.
Garzoli S., Parisi V., Paschini E., 1981. On the effect of bottom topography on two eddies in the Sardinia and Sicily region, *Deep-Sea Res.*, **29**, 77-86.
Gill A. E., 1977. The hydraulics of rotating-channel flow, *J. Fluid Mech.*, **80**, 641-671.
Gill A., Schumann E. H., 1979. Topographically induced changes in the structure of an inertial coastal jet. Application to the Agulhas Current, *J. Phys. Oceanogr.*, **9**, 975-991.
Hogg N., 1983. Hydraulic control and flow separation in a multilayered fluid with applications to the Vema Channel, *J. Phys. Oceanogr.*, **13**, 695-708.
Lacombe M., 1971. Le détroit de Gibraltar, océanographie physique, Notes M. Serr. Geol. Maroc., M222 bis, 111-146.
Morel A., 1969. Résultats des observations effectuées dans le détroit de Sicile, *Cah. Océanogr.*, **21**, 2, 203-244.
Nof D., 1978 *a*. On geostrophic adjustment in sea straits and wide estuaries: theory and laboratory experiments. Part I: One-layer system, *J. Phys. Oceanogr.*, **8**, 690-702.
Nof D., 1978 *b*. On a geostrophic adjustment in sea straits and wide estuaries: theory and laboratory experiments. Part II: Two-layer system, *J. Phys. Oceanogr.*, **8**, 861-872.
Rydberg L., 1980. Rotating hydraulics in deep-water channel flow, *Tellus*, **32**, 77-89.
Stocchino C., Testoni A., 1969. Le correnti nel Canale di Corsica e nell'Arcipelago Toscano, *Comm. Ital. Oceanogr.*, **827** A, 19.
Whitehead J. A., Leetmaa A., Knox R. A., 1974. Rotating hydraulics of strait and sill flows, *Geophys. Fluid Dyn.*, **6**, 101-125.

APPENDIX

Calling

$$\gamma_{r(l)} = 2 d_1^{\infty} \left(\frac{d_1^{\infty}}{d_{1\,r(l)}^{\infty}} - 1 \right)$$

and

$$\Delta_{r(l)} = \frac{2\rho}{\Delta\rho} d_1^{\infty} (\xi^{\infty} - \xi_{r(l)}^{\infty})$$

equations (21), (22) can be written as:

$$a^2 \operatorname{sh}^2\left(\frac{L}{R}\right) + b^2 \operatorname{ch}^2\left(\frac{L}{R}\right) + 2ab \operatorname{sh}\left(\frac{L}{R}\right) \operatorname{ch}\left(\frac{L}{R}\right) - a\gamma_r \operatorname{ch}\left(\frac{L}{R}\right) - b\gamma_r \operatorname{sh}\left(\frac{L}{R}\right) + \Delta_r = 0$$

$$a^2 \operatorname{sh}^2\left(\frac{L}{R}\right) + b^2 \operatorname{ch}^2\left(\frac{L}{R}\right) - 2ab \operatorname{sh}\left(\frac{L}{R}\right) \operatorname{ch}\left(\frac{L}{R}\right) + a\gamma_l \operatorname{ch}\left(\frac{L}{R}\right) - b\gamma_l \operatorname{sh}\left(\frac{L}{R}\right) - \Delta_l = 0.$$

After some algebra, with the position:

$$\Gamma_+ = \gamma_r + \gamma_l, \qquad \Delta_+ = \Delta_r + \Delta_l$$
$$\Gamma_- = \gamma_r - \gamma_l, \qquad \Delta_- = \Delta_r - \Delta_l,$$

we obtain:

$$a=\frac{b\Gamma_- \operatorname{sh} L/R-\Delta}{(4b \operatorname{sh}(L/R)-\Gamma_-)\operatorname{ch}(L/R)}, \qquad \text{(A1)}$$

corresponding to a quartic equation in the unknown b:

$$\alpha b^4+\beta b^3+Qb^2+\lambda b+\varepsilon=0$$
$$b\neq\frac{\Gamma_-}{4 \operatorname{sh}(L/R)}, \qquad \text{(A2)}$$

where:

$$\alpha=32 \operatorname{sh}^2(L/R) \operatorname{ch}^2(L/R)$$
$$\beta=-16\Gamma_+[\operatorname{ch}^2(L/R)+\operatorname{sh}^2(L/R)] \operatorname{sh}(L/R)$$
$$\varphi=2\{\Gamma_-^2[\operatorname{tgh}^2(L/R)-2] \operatorname{sh}^2(L/R)$$
$$+\Gamma_+^2[\operatorname{ch}^2(L/R)+4 \operatorname{sh}^2(L/R)]$$
$$-8\Delta_- \operatorname{sh}^2(L/R)\}$$
$$\lambda=\{\Gamma_+(\Gamma_-^2-\Gamma_+^2)$$
$$+4\Gamma_-\Delta_+\frac{1}{\operatorname{ch}^2(L/R)}+8\Gamma_+\Delta_-\} \operatorname{sh}(L/R)$$
$$\varepsilon=2\Delta_+^2 \operatorname{tgh}^2(L/R)-\Gamma_+(\Gamma_-\Delta_++\Gamma_+\Delta_-)$$

Simple mathematical solutions at the (A1)–(A2) can be found in the following cases:

a) $\Gamma_+=\Gamma_-=0$, *e.g.* $d_1^\infty=d_{1r}^\infty=d_{1l}^\infty$

$$a=\mp\frac{\Delta_+}{2 \operatorname{sh}(L/R)\sqrt{\Delta_-\pm\sqrt{\Delta_-^2-\Delta_+^2}}};$$

$$b=\pm\frac{\sqrt{\Delta_-\pm\sqrt{\Delta_-^2\Delta_+^2}}}{2 \operatorname{ch}(L/R)}$$

b) $\Gamma_+=\Delta_+=0$

$$a=\frac{\gamma_r}{2\operatorname{ch}(L/R)};$$

$$b=\pm\frac{\gamma_r}{2\operatorname{ch}(L/R)}\sqrt{\frac{4\Delta_r}{\gamma_r^2}+[2-\operatorname{tgh}^2(L/R)]}$$

c) $\Gamma_+=\Gamma_-=0=\Delta_+$, *e.g.* $d_1^\infty=d_{1r}^\infty=d_{1l}^\infty$ and $\Delta_-=2\Delta_r$

$$a=0; \qquad b=\pm\frac{\sqrt{\Delta_r}}{2\operatorname{ch}(L/R)}.$$

In this way:

$$Q=Q^\infty \operatorname{tgh}(L/R)$$

with:

$$Q^\infty=\pm\frac{2g'd_1^\infty}{f_0}\sqrt{\frac{2\rho}{\Delta\rho}d_1^\infty(\xi^\infty-\xi_r^\infty)}$$
$$d_1=d_1^\infty+\frac{Q^\infty}{2f_0R^2}\frac{\operatorname{sh}(x/R)}{\operatorname{ch}(L/R)}$$
$$v_1=\frac{Q^\infty}{2Rd_1^\infty}\frac{\operatorname{ch}(x/R)}{\operatorname{ch}(L/R)}$$